
Learning State Representations from Random Deep Action-conditional Predictions

Zeyu Zheng¹ Vivek Veeriah¹ Risto Vuorio^{1†} Richard Lewis¹ Satinder Singh¹

Abstract

In this work, we study auxiliary *prediction* tasks defined by *temporal-difference networks* (TD networks) (Sutton & Tanner, 2004); these networks are a language for expressing a rich space of general value function (GVF) prediction targets that may be learned efficiently with TD. Through analysis in an illustrative domain we show the benefits to learning state representations of exploiting the full richness of TD networks, including both action-conditional predictions and temporally deep predictions. Our main (and perhaps surprising) result is that deep action-conditional TD networks with random structures that create random prediction-questions about random features yield state representations that are competitive with state-of-the-art hand-crafted value prediction and pixel control auxiliary tasks in both Atari games and DeepMind Lab tasks. We also show through stop-gradient experiments that learning the state representations *solely* via these unsupervised random TD network prediction tasks yield agents that outperform the end-to-end-trained actor-critic baseline.

1. Introduction

Providing auxiliary tasks to Deep Reinforcement Learning (Deep RL) agents has become an important class of methods for driving the learning of representations that accelerate learning on a main task. Existing auxiliary tasks have the property that their *semantics* are fixed and carefully designed by the agent designer. Some notable examples include pixel control, reward prediction, termination prediction, and multi-horizon value prediction (these are reviewed in more detail below). Unlike the prior approaches that require careful design of auxiliary task semantics, we explore here a different approach in which a set of *random prediction tasks* are generated through a rich space of

general value functions (GVFs) defined by a language of predictions of random features of observations. We adopt *temporal-difference networks* (TD networks) (Sutton & Tanner, 2004) as our language of GVF prediction targets. Our main, and perhaps surprising, result is that TD networks that ask *random questions* about the action-conditional futures of *random features* yield state representations that are competitive with state-of-the-art auxiliary tasks with hand-crafted semantics. We demonstrate this in Atari games and DeepMind Lab tasks, comparing to multi-horizon value prediction and pixel control as our baseline auxiliary tasks.

Through empirical analyses on illustrative domains we show the benefits of exploiting the richness of TD networks—their temporal depth and action-conditionality. We also provide direct evidence that using random TD networks learns useful representations for the main task through a set of *stop-gradient* experiments in which the state representations are trained *solely* via the random TD network tasks without using the rewards. We show that—again, surprisingly—these stop-gradient agents outperform the end-to-end-trained actor-critic baseline.

2. Related Work

Auxiliary tasks were formalized and introduced to RL by Sutton et al. (2011) through the Horde learning architecture. Horde is an off-policy learning framework for learning knowledge from an agent’s experience. This knowledge was in the form of predictions represented as a set of GVFs. Our work is related to Horde in that TD networks express a rich subspace of GVFs but differs from Horde in that our interest is in the effect of learning these auxiliary predictions on the main task via shared state representations (as opposed to the knowledge captured in these GVFs). Our work is also related to predictive state representations (PSRs) (Littman et al., 2001; Singh et al., 2004). PSRs use predictions *as* state representations whereas our work learns latent state representations from predictions. Recently, in the use of deep neural networks in RL as powerful function approximators, various auxiliary tasks have been proposed to improve the latent state representations of Deep RL agents. We review these auxiliary tasks below. Our work belongs to this family of work in that the auxiliary prediction tasks are used

[†]Now at the University of Oxford. ¹University of Michigan. Correspondence to: Zeyu Zheng <zeyu@umich.edu>.

to improve the state representations of Deep RL agents.

All of the following approaches in this paragraph have *pre-defined* GVF targets for the auxiliary task predictions. *UNREAL* (Jaderberg et al., 2017) uses reward prediction (and also an auxiliary pixel control task) and achieved a significant performance improvement in DeepMind Lab but only marginal improvement in Atari. Kartal et al. (2019) found predicting episode termination an useful auxiliary task in episodic RL settings. However, they only demonstrated mild improvement in four Atari games. SimCore DRAW (Gregor et al., 2019) learns a generative model of future observations conditioned on action sequences and uses it as an auxiliary task to shape the agent’s belief states in partially observable environments. Fedus et al. (2019) found that simply predicting the return with multiple different discount factors (MHVP) serves as an effective auxiliary task. MHVP relies on the availability of rewards and thus is different from our work and other unsupervised auxiliary tasks.

The following approaches use information-theoretic methods to learn good representations that are informative about the future trajectory of these representations as the agent interacts with the environment. CPC (van den Oord et al., 2018), CPA|action (Guo et al., 2018), ST-DIM (Anand et al., 2019), and DRIML (Mazouze et al., 2020) apply different forms of temporal contrastive losses to learn predictions in a latent space. PBL (Guo et al., 2020) focuses on partially observable environments and introduces a separate target encoder to set the prediction targets. The target encode is trained to distill the learned state representations. SPR (Schwarzer et al., 2020) replaces the target encoder in PBL with a moving average of the state representation function. In addition to being predictive, PI-SAC (Lee et al., 2020) also enforces the state representations to be compressed. SPR and PI-SAC focuses on data efficiency and only conducted experiments under low data budgets. In the works cited in this paragraph the targets are not GVFs and despite some empirical success, none of these works could learn long-term predictions effectively. This is in contrast to GVF-like prediction tasks which can be effectively learned via TD as in our work as well as the work presented in the previous paragraph.

Bellemare et al. (2019) and Dabney et al. (2020) studied the optimal representation in RL from a geometric perspective and provided theoretical insights into why predicting GVF-like targets is helpful in learning state representations. Our work is consistent with this theoretical motivation.

In a recent work, Veeriah et al. (2019) used metagradients to discover very simple kinds of GVFs (essentially discounted sums of features of observations) instead of hand-crafting them. In this work, we explore a much richer space of GVFs and show that random choices of features and random but rich GVFs are competitive with the state of the art of hand-

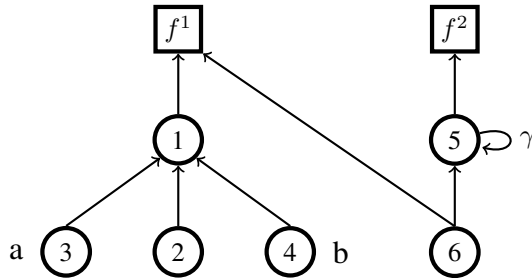


Figure 1. An example of a question network. The squares represent *feature nodes* and circles represent the *prediction nodes*. Description about question network is in § 3.1.

crafted GVFs as auxiliary tasks.

3. Method

In this section we first describe the TD networks formalism for defining GVFs, then we describe RADAR, our procedure for constructing random GVFs, and then finish this section with a description of the agent architecture used in our empirical work.

3.1. Background on TD Networks

A TD network is a graph in which the nodes represent predictions. In the original work, there are two sets of edges in a TD network. One set defines the targets of the predictions and the graph formed by those edges is called the *question network*. The other set determines the computational process for computing the predictions and is called the *answer network*. In this work we are only interested in question network part of a TD network because it defines the prediction-semantics or targets. We do not use the answer network; instead we parameterize the computation of the predictions using a deep neural network and update the predictions via backpropagation.

Figure 1 shows an example of a question network. The two squares represent two *feature nodes* and the six circles represent six *prediction nodes*. Node 1 (labeled in the circles) predicts the expected value of feature f^1 at the next step. Implicitly, this prediction is conditioned on following the current policy. Node 2 predicts the expected value of node 1 at the next step. Note that we can “unroll” the target of node 2 to ground it on the features. In this example, node 2 predicts the expected value of feature f^1 after two steps when following the current policy. Node 5 has a self-loop and predicts the expectation of the discounted sum of feature f^2 with a discount factor γ . We will call this a *conventional TD prediction* except that it is a general value function because the feature f^2 is not the reward but some other function of observation. Node 3 is labeled by action a . It predicts the expected value of node 1 at the next step given action a is

taken at the current step. We say node 3 is *conditioned* on action a . Similarly, node 4 predicts the same target but is conditioned on action b . Node 6 has two outgoing links. It predicts the *sum* (in general weighted sum, but in this paper we do not explore the role of these weights and instead fix them to be 1) of feature f^1 and the value of node 5, both at the next step. In this case, it is hard to describe the semantic of node 6’s prediction in terms of the features, but we can see that the prediction is still grounded on feature f^1 and f^2 .

Generalising from the example above, a question network with n_p prediction nodes and n_f feature nodes defines n_p predictions of n_f features. We use N_p to denote the set of all prediction nodes and N_f to denote the set of all feature nodes. Let W be the adjacency matrix of the question network. W_{ij} denotes the weight on the edge from node i to node j . We define $W_{ij} \triangleq 0$ if there is no edge from node i to node j . Now consider an agent interacting with the environment. At each step t , it receives an observation O_t and takes an action A_t according to its policy π . Then at the next step it receives an observation O_{t+1} . The feature $f^k(O_t, A_t, O_{t+1})$ is a scalar function of the transition. The agent makes a prediction $y^i(O_0, A_0, \dots, O_t)$ for each prediction node i based on its history; this is computed by a neural network in our work. For brevity, we use f_{t+1}^k and y_t^i to denote $f^k(O_t, A_t, O_{t+1})$ and $y^i(O_0, A_0, \dots, O_t)$ respectively. The target for prediction i at step t is denoted by z_t^i . If prediction node i is not conditioned on any action, its target is

$$z_t^i = \mathbb{E}_\pi \left[\sum_{j \in N_p} W_{ij} z_{t+1}^j + \sum_{k \in N_f} W_{ik} f_{t+1}^k \right]$$

otherwise, if it is conditioned on action a^i , its target is

$$z_t^i = \mathbb{E}_\pi \left[\sum_{j \in N_p} W_{ij} z_{t+1}^j + \sum_{k \in N_f} W_{ik} f_{t+1}^k \mid A_t = a^i \right].$$

By the construction of the targets, the agent can learn the prediction y_t^i via TD. If i is not conditioned on any action, then y_t^i is updated by

$$y_t^i \leftarrow \sum_{j \in N_p} W_{ij} y_{t+1}^j + \sum_{k \in N_f} W_{ik} f_{t+1}^k$$

otherwise, if i is conditioned on action a^i , then y_t^i is updated by

$$y_t^i \leftarrow \begin{cases} \sum_{j \in N_p} W_{ij} y_{t+1}^j + \sum_{k \in N_f} W_{ik} f_{t+1}^k & \text{if } A_t = a^i \\ y_t^i & \text{otherwise} \end{cases}$$

In an episodic setting, if the episode terminates at step T , we define $z_T^i \triangleq 0$ and $y_T^i \triangleq 0$ for all prediction nodes i .

TD networks represent a broader class of predictions than the conventional value functions. Many existing predictions used as auxiliary tasks can be expressed by a question network. Reward prediction (Jaderberg et al., 2017) can be represented by a question network with a single feature node representing the reward and a single prediction node predicting the reward. Multi-horizon value prediction (Fedus et al., 2019) can be represented by a similar question network but with multiple self-loop prediction nodes with different discount factors. Termination prediction (Kartal et al., 2019) can be represented by a question network with a feature node of constant 1 and a self-loop node with discount 1.

3.2. A Random Question Network Generator

In this work, instead of hand-crafting a new question network instance as in previous work on the use of predictions for auxiliary tasks, we verify a conjecture that a large number of random deep, action-conditional predictions is enough to drive the learning of good state representations without needing to carefully hand-design the semantics of those predictions. To test this conjecture, we designed a generator of random question networks from which we can take samples and evaluate their performance as auxiliary tasks. Specifically, we designed **R**andom **D**eep **A**ction-conditional **p**redictions (RADAR), a heuristic algorithm that generates question networks with random structures.

Random Features. RADAR uses random features, each computed by a scalar function g^k with random parameters. For any transition (O_t, A_t, O_{t+1}) , the feature for this transition is computed as $f_{t+1}^k = |g^k(O_{t+1}) - g^k(O_t)|$. Instead of directly using the output of g^k as the feature, we use the amount of change in g^k . A similar transformation was used in the pixel control auxiliary task (Jaderberg et al., 2017).

Random Structure. The question network structure in RADAR is defined with 5 arguments as input - number of features n_f , the discrete action set \mathcal{A} , a discount factor γ , depth D , and repeat R ; its output is a question network that contains n_f feature nodes as defined above, and $D + 1$ layers, each layer contains $R \times |\mathcal{A}|$ prediction nodes except the first layer which contains n_f prediction nodes. RADAR constructs the question network layer by layer incrementally from layer 0 to layer D . Layer 0 has n_f feature nodes and n_f prediction nodes; each prediction node has an edge to a distinct feature node with weight 1 on the edge and has a self-loop with weight γ . Each prediction node in layer 0 predicts the discounted sum of its corresponding feature node at the next step and are not conditioned on actions. The procedure for generating each layer from 1 through D is the same. For a layer l ($1 \leq l \leq D$), RADAR creates $R \times |\mathcal{A}|$ prediction nodes. Each prediction node is conditioned on one action and there are exactly R nodes that are conditioned on the same action. Each prediction node has two edges,

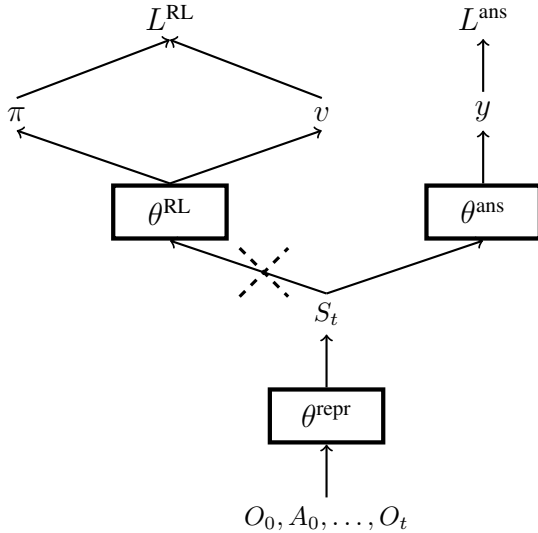


Figure 2. The agent architecture. The dashed cross denotes an optional stop-gradient operation.

one to a random node in layer $l - 1$ and one to a random feature node in layer 0. Note that prediction nodes in layer 1 do not necessarily connect to a prediction node in layer 0 - they may only connect to a feature node. A constraint for preventing duplicated predictions is included in RADAR so that any two prediction nodes in layer l that are conditioned on the same action cannot connect to the same prediction node in layer $l - 1$. Detailed pseudocode for RADAR is provided in the Appendix.

3.3. Agent Architecture

Figure 2 shows the agent architecture. We base our agent on the actor-critic architecture and it consists of 3 modules. The state representation module, parameterized by θ^{repr} , maps the history of observations and actions (O_0, A_0, \dots, O_t) to a state vector S_t . The RL module, parameterized by θ^{RL} , maps the state vector S_t to a policy distribution over the available actions $\pi(\cdot|S_t)$ and a value function $v(S_t)$. The answer network module, parameterized by θ^{ans} , maps the state vector S_t to a set of predictions $y(S_t)$ equal in size to the number of prediction nodes in the question network.

We trained the network in two separate ways. In the auxiliary task setting, the RL loss \mathcal{L}^{RL} is backpropagated to update the parameters of the state representation (θ^{repr}) and the RL (θ^{RL}) modules, while the answer network loss \mathcal{L}^{ans} is backpropagated to update the parameters of the answer network (θ^{ans}) and state representation (θ^{repr}) modules. Note that the answer network loss only affects the RL module indirectly through the shared state representation module. In the stop-gradient setting, we stopped the gradients from the RL loss from flowing from \mathcal{L}^{RL} to θ^{repr} . This allows us to do a harsher and more direct evaluation of how well the

auxiliary tasks can train the state representation without any help from the main task.

For \mathcal{L}^{RL} , we used the standard actor-critic objective with an entropy regularizer (Mnih et al., 2016). For \mathcal{L}^{ans} , we used the mean-squared loss for all the targets and predictions.

4. Illustrating the Benefits of Deep Action-conditional Questions

We present our experiments and analyses in two sections. The main aim of the experiments in this section is to explore the benefits of exploiting the full richness of the space defined by TD networks, by systematically varying the depth, features, and action-conditional of the question networks. We illustrate the benefits first in a simple grid world that affords the use of intuitive features and visualizations, and then on a set of six Atari games. In addition, to test the robustness of RADAR to its hyperparameters, we conducted a random search experiment on the Atari game Breakout.

4.1. Benefits of Depth: Illustrative Grid World

Although our primary interest (and the focus of subsequent experiments) is learning good policies, in this domain we study *policy evaluation* because this simpler objective is sufficient to illustrate our points and we can compute and visualize the true value function for comparison. Figure 3a shows the environment, a 7 by 7 grid surrounded by walls. The observation is a $9 \times 9 \times 3$ top-down view including the walls. 3 channels represent the walls, the agent, and the goal. There are 4 available actions that move the agent horizontally or vertically to an adjacent cell. The agent gets a reward of 1 upon arriving at the goal cell located in the top row, and 0 otherwise. This is a continuing environment so achieving the goal does not terminate the interaction. The objective here is to learn the state-value function of a *random policy* which selects each action with equal probability. We used a discount factor of 0.98.

Specifying a question network requires specifying both the structure and the features. Later we explore random features, but here we use a single hand-crafted `touch` feature so that every prediction has a clear semantics. `touch` is 1 if the agent’s move is blocked by the wall and is 0 otherwise.

Using the `touch` feature we constructed two types of question networks. The first type is the expected discounted sum of `touch` (we used a discount factor 0.8). We refer to this as a *conventional TD prediction target* (Figure 3b). The second type is a *full action-conditional tree* of depth D . There is only one feature node in the tree which corresponds to the `touch` feature. Each internal node has 4 child nodes conditioned on distinct actions. Each prediction node also has a skip edge directly to the feature node (except for the child nodes of the feature node). Figure 3c shows an exam-

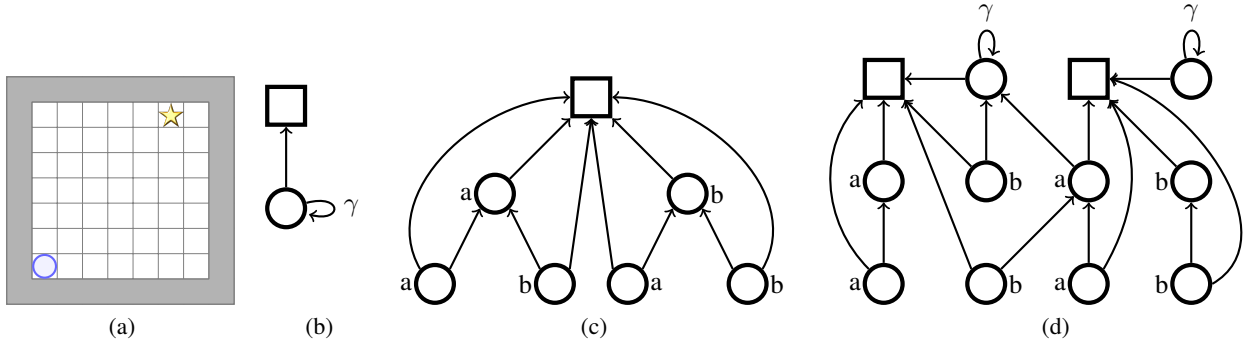


Figure 3. Empty room grid world environment and the question networks we studied in our illustrative experiment. (a) The blue circle denotes the agent and the yellow star denotes the rewarding state. (b) A conventional TD prediction. (c) A depth-2 tree question network with 2 actions. The bottom right prediction node predicts the sum of the values of the feature in the next two steps if action b were taken for both the current and the next step. Other prediction nodes have similar semantics. (d) A random question network sampled from RADAR. There are 2 features and 2 actions, with depth and repeat set to 2.

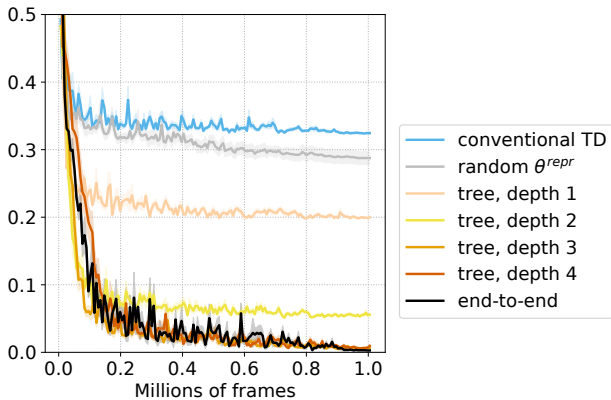


Figure 4. MSE between the learned value function and the true value function in the tree question networks experiment in the empty room grid world environment. The agent trained with action-conditional question networks (tree, depth = 1, 2, 3, 4) achieved substantially lower MSE than the random baseline and the agent trained with conventional TD prediction target. The performance improved monotonically with increasing depth until depth 3, where the performance matched to that of end-to-end training (black curve). Each curve is averaged over 10 independent runs with different random seeds. Shaded area shows the standard error.

ple of a depth-2 tree (the caption describes the semantics of some of the predictions). We also compared to a randomly initialized state representation module as a baseline where the state representation was fixed and only the value function weights were learned during training.

Neural Network Architecture. The empty room environment is fully observable and so the state representation module is a feed-forward neural network that maps the current observation O_t to a state vector S_t . It is parameterized by a 3-layer multi-layer perceptron (MLP) with 64 units in the first two layers and 32 units in the third layer. The RL mod-

ule has one hidden layer with 32 units and one output head representing the state value. (There is no policy head as the policy was given). The answer network module also has one hidden layer with 32 units and one output layer. We applied a stop-gradient between the state representation module and the RL module (Figure 2). More implementation details are provided in the Appendix.

Results. We measured the performance by the mean-squared error (MSE) between the learned value function and the true value function across all states. The true value function was obtained by solving a system of linear equations (Sutton & Barto, 2018). Figure 4 shows the MSE during training. Both the random baseline and the conventional TD prediction target performed poorly. But even a tree question network of depth 1 (i.e., four prediction targets corresponding to the four action conditional predictions of `touch` after one step) performed much better than these two baselines. Performance increased monotonically with increasing depth until depth 3 when the MSE matched end-to-end training after 1 million frames.

Figure 5 shows the different value functions learned by agents with the different prediction tasks. Figure 5a visualizes the true value function. Figure 5b shows the learned value function when the state representations are learned from conventional TD predictions of `touch`. Its symmetric pattern reflects the symmetry of the grid world and the random policy, but this is inconsistent with the asymmetric true value function. Figure 5c shows the learned value function when the state representations are learned from depth-1-tree predictions. It clearly distinguishes 4 corner states, 4 groups of states on the boundary, and the states in the center area, because this grouping reflects the different prediction targets for these states.

For the answer network module to make accurate predictions of the targets of the question network, the state representa-

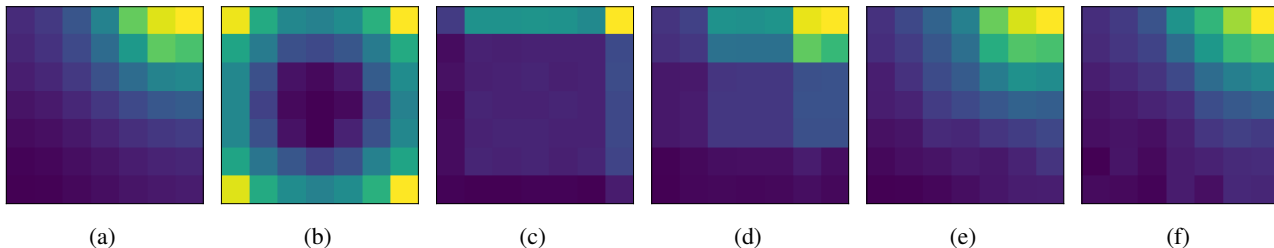


Figure 5. Visualization of the learned value functions in the empty room environment. Bright indicates high value and dark indicates low value. (a) The true values. (b) The conventional TD predictions of the `touch` feature. (c) - (f) The prediction are defined by a full-tree-structured question network regarding the `touch` feature. The depth of the tree increases from 1 to 4 from (c) to (f).

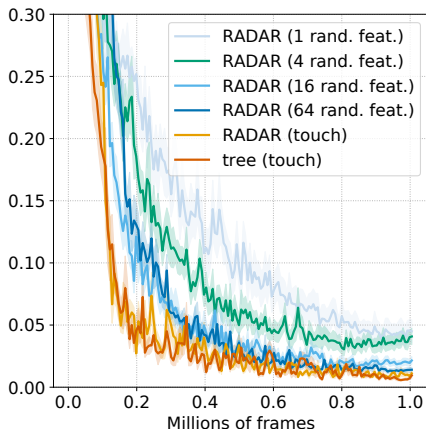


Figure 6. MSE between the learned value function and the true value function in the random question networks experiment in the empty room environment. Different loss curves show the performance of agents trained with different RADAR variants. Increasing the number of random features (from 1 to 64) improves the performance. Each curve is averaged over 10 independent runs with different random seeds. Shaded area shows the standard error.

tion module must map states with the same prediction target to similar representations and states with different targets to different representations. As the question network tree becomes deeper, the agent learns finer state distinctions, until an MSE of 0 is achieved at depth 3 (Figure 5e).

4.2. Benefits of Random Question Nets: Illustrative Grid World

The previous experiment demonstrated benefits of temporally deeper prediction tasks. But achieving this by creating deeper and deeper full-branching action-conditional trees is not tractable as the number of prediction targets grows exponentially. The previous experiment also used a single feature formulated using domain knowledge; such feature selection is also not scalable. RADAR provides a method to mitigate both concerns by growing random question networks with random features.

Specifically, we used RADAR with *discount* 0.8, *depth* 4, and *repeat* equal to the number of features. Figure 6 shows the MSE of different RADAR variants. The performance of RADAR with `touch`—that is, random but not necessarily full branching trees of depth 4—performed as well as `touch` with a full tree of depth 4. RADAR with a single random feature performed suboptimally; a random feature is likely less discriminative than `touch`. However, as the number of random features increases, the performance improves, and with 64 random features, RADAR matches the final performance of `touch` with a full depth 4 tree.

The results on the grid world provide preliminary evidence that RADAR-generated deep random question networks with many random features can yield good state representations. We next test this conjecture on a set of Atari games, exploring again the benefits of depth and also exploring the benefit of action conditionality.

4.3. Benefits of Action Conditionality and Depth: Atari

Here we use six Atari games (these six are often used for hyperparameter selection for the Atari benchmark (Mnih et al., 2016)) to compare four different question networks: (a) *Conventional TD* predictions of discounted sums of distinct random features (Figure 3b); (b) *Shallow action-conditional* predictions, a set of depth-1 trees, each for a distinct random feature (Figure 3c); (c) RADAR without action-conditioning; and (d) RADAR (Figure 3d). Network (a) provides a useful TD-prediction baseline that exploits none of the richness of TD networks; the contrast between (b) and (c) provides further evidence for the benefits of depth; and the contrast between (c) and (d) provides evidence of the benefits of conditioning predictions on actions.

Random Features for Atari. The random function g for computing the random features are designed as follows. The 84×84 observation O_t is divided into 16 disjoint 21×21 patches, and a *shared* random linear function applies to each patch to obtain 16 random features $g_t^1, g_t^2, \dots, g_t^{16}$. Finally, we process these features as described in §3.2.

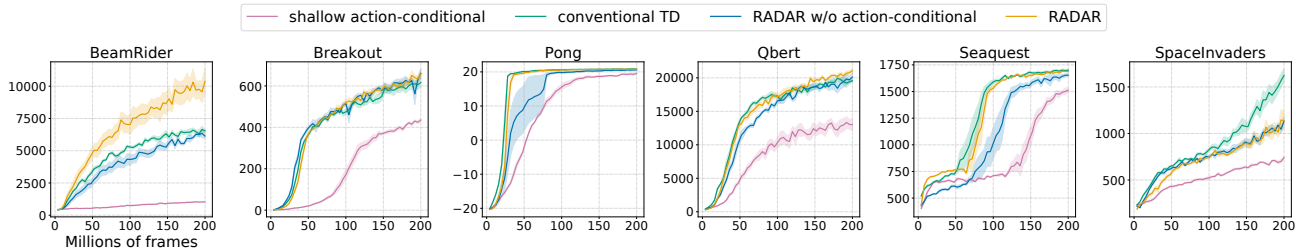


Figure 7. Learning curves of different question networks in six Atari games. x-axis denotes the number of frames and y-axis denotes the episode returns. Each curve is averaged over 5 independent runs with different random seeds. Shaded area shows the std. error.

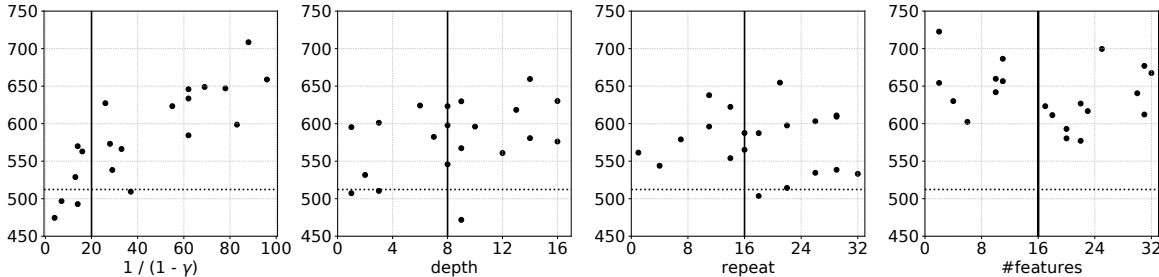


Figure 8. Scatter plots of scores in Breakout obtained by RADAR with different hyperparameters. x-axis denotes the value of the hyperparameter. y-axis denotes the final game score after training for 200 million frames. The dotted horizontal lines denote the performance of the end-to-end A2C baseline. The solid vertical lines denote the values we used in our final experiments.

Neural Network Architecture. We used A2C (Mnih et al., 2016) with a standard neural network architecture for Atari (Mnih et al., 2015) as our base agent. Specifically, the state representation module consists of 3 convolutional layers. The RL module has one hidden dense layer and two output heads for the policy and the value function respectively. The answer network has one hidden dense layer with 512 units followed by the output layer. We stopped the gradient from the RL module to the state representation module (Figure 2).

Hyperparameters. The discount factor, depth, and repeat for RADAR were set to 0.95, 8, and 16 respectively. Thus there are $16 + 8 * 16 * |\mathcal{A}|$ total predictions. RADAR without action-conditioning has the same question network as RADAR except that no prediction was conditioned on actions. To match the total number of predictions, we used $16 + 8 * 16 * |\mathcal{A}|$ random features for conventional TD and $8 * 16$ features for shallow action-conditional predictions. Additional random features were generated by applying more random linear functions to the image patches. The discount factor for conventional TD predictions is also 0.95. More implementation details are provided in the Appendix.

Results. Figure 7 shows the learning curves in the 6 Atari games. Shallow action-conditional predictions performed the worst in all the games, providing further evidence for the value of making deep predictions. RADAR consistently outperformed its non-action-conditional counterpart, providing clear evidence that action-conditioning is beneficial.

And finally, RADAR performed better than conventional TD predictions in 5 out of 6 games despite using many fewer features, suggesting that structured deep action-conditional predictions can be more effective than simply making conventional TD predictions about many features.

4.4. Robustness and Stability

We tested the robustness and stability of RADAR with respect to its hyperparameters, namely discount, depth, repeat, and number of features. We explored different values for each hyperparameter independently while holding the other hyperparameters fixed to the values we used in the previous experiment. For each hyperparameter, we took 20 samples uniformly from a wide interval and evaluated RADAR on Breakout using the sampled value. The results are presented in Figure 8. Each hyperparameter has a range of values that achieves high performance, indicating that RADAR is stable and robust to different hyperparameter choices.

5. Comparison to Baseline Auxiliary Tasks on Atari and DeepMind Lab

In this section, we present the empirical results of comparing the performance of RADAR against the A2C baseline (Mnih et al., 2016) and two other auxiliary tasks, i.e., multi-horizon value prediction (MHVP) (Fedus et al., 2019) and pixel control (PC) (Jaderberg et al., 2017). We conducted the evaluation in 49 Atari games and 12 DeepMind

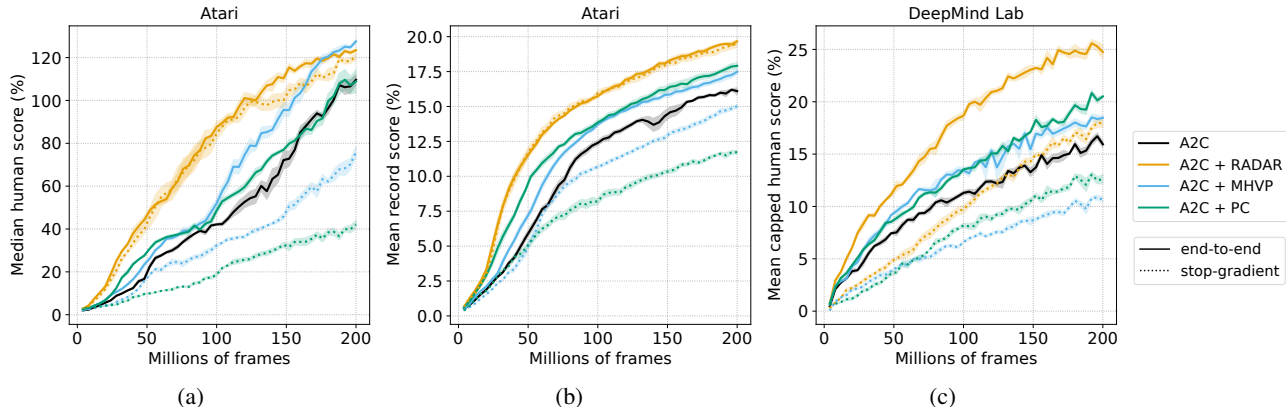


Figure 9. (a) Median human-normalized score across 49 Atari games. (b) Mean record-normalized score across 49 Atari games. (c) Mean capped human-normalized score across 12 DeepMind Lab environments. In all panels, the x-axis denotes the number of frames. Each dark curve is averaged over 5 independent runs with different random seeds. The shaded area shows the standard error.

Lab environments.

Atari Implementation. For Atari games, we used the same architecture for RADAR as in the prior section. For MHVP, we used 10 value predictions following (Fedus et al., 2019). Each prediction has a unique discount factor, chosen to be uniform in terms of their effective horizons from 1 to 100 ($\{0, 1 - \frac{1}{10}, 1 - \frac{1}{20}, \dots, 1 - \frac{1}{90}\}$). The architecture for MHVP is the same as RADAR. For PC, we followed the architecture design and hyperparameters in (Jaderberg et al., 2017). When not stopping gradient from the RL loss, we mixed the RL updates and the answer network updates by scaling the learning rate for the answer network with a coefficient c . We searched c in $\{0.1, 0.2, 0.5, 1, 2\}$ on the 6 games in the previous section. $c = 1$ worked the best for all methods. More details are provided in the Appendix.

DeepMind Lab Implementation. For DeepMind Lab, we used the same RL module and answer network module as Atari but used a different state representation module to address the partial observability. Specifically, the convolutional layers in the state representation module were followed by a dense layer with 512 units and a GRU core (Cho et al., 2014; Chung et al., 2014) with 512 units.

Results. Figure 9a and Figure 9b shows the results for both the stop-gradient and end-to-end architectures on Atari, comparing to two standard human-normalized score measures (median human-normalized score (Mnih et al., 2015) and mean record-normalized score (Hafner et al., 2020)). When training representations end-to-end through a combined main task and auxiliary task loss, the performance of RADAR matches or substantially exceeds the two baselines. Surprisingly, the stop-gradient RADAR agents outperform the end-to-end A2C baseline, unlike stop-gradient versions of the baseline auxiliary task agents. Figure 9c shows the results for both stop-gradient and end-to-end ar-

chitectures on 12 DeepMind Lab environments (using mean capped human-normalized scores). Again, RADAR substantially outperforms both auxiliary task baselines, and the stop-gradient version matches the final performance of the end-to-end A2C. Taken together the results from these 61 tasks provide substantial evidence that RADAR-generated random question networks drive the learning of good state representations, outperforming auxiliary tasks with fixed hand-crafted semantics.

6. Conclusion and Future Work

In this work we provided evidence that learning how to make random, deep action-conditional predictions can drive the learning of good state representations. We used the language of TD networks to define a rich space of predictions that can be learned efficiently with TD methods, and created a heuristic algorithm, RADAR, that generates prediction targets in this space that take the form of random question networks with random features. Our empirical study on the Atari and DeepMind Lab benchmarks shows that learning state representations solely via auxiliary prediction tasks defined by RADAR outperforms the end-to-end trained A2C baseline. RADAR also outperformed pixel control and multi-horizon value prediction on these two benchmarks when being used as part of a combined loss function with the main RL task.

In this work, the question network was sampled before learning and was held fixed during learning. An interesting goal for future research is to find methods that can adapt the question network and discover useful questions during learning. The question networks we studied are limited to discrete actions. It is unclear how to condition a prediction on a continuous action. Thus another future direction to explore is to extend TD networks to continuous action spaces.

Acknowledgement

This work was supported by DARPA’s L2M program as well as a grant from the Open Philanthropy Project to the Center for Human Compatible AI. Any opinions, findings, conclusions, or recommendations expressed here are those of the authors and do not necessarily reflect the views of the sponsors.

References

- Anand, A., Racah, E., Ozair, S., Bengio, Y., Côté, M., and Hjelm, R. D. Unsupervised state representation learning in atari. In Wallach, H. M., Larochelle, H., Beygelzimer, A., d’Alché-Buc, F., Fox, E. B., and Garnett, R. (eds.), *Advances in Neural Information Processing Systems 32: Annual Conference on Neural Information Processing Systems 2019, NeurIPS 2019, December 8-14, 2019, Vancouver, BC, Canada*, pp. 8766–8779, 2019.
- Bellemare, M. G., Dabney, W., Dadashi, R., Taïga, A. A., Castro, P. S., Roux, N. L., Schuurmans, D., Lattimore, T., and Lyle, C. A geometric perspective on optimal representations for reinforcement learning. In Wallach, H. M., Larochelle, H., Beygelzimer, A., d’Alché-Buc, F., Fox, E. B., and Garnett, R. (eds.), *Advances in Neural Information Processing Systems 32: Annual Conference on Neural Information Processing Systems 2019, NeurIPS 2019, December 8-14, 2019, Vancouver, BC, Canada*, pp. 4360–4371, 2019.
- Cho, K., van Merriënboer, B., Bahdanau, D., and Bengio, Y. On the properties of neural machine translation: Encoder-decoder approaches. In Wu, D., Carpuat, M., Carreras, X., and Vecchi, E. M. (eds.), *Proceedings of SSST@EMNLP 2014, Eighth Workshop on Syntax, Semantics and Structure in Statistical Translation, Doha, Qatar, 25 October 2014*, pp. 103–111. Association for Computational Linguistics, 2014. doi: 10.3115/v1/W14-4012.
- Chung, J., Gülçehre, Ç., Cho, K., and Bengio, Y. Empirical evaluation of gated recurrent neural networks on sequence modeling. *CoRR*, abs/1412.3555, 2014.
- Dabney, W., Barreto, A., Rowland, M., Dadashi, R., Quan, J., Bellemare, M. G., and Silver, D. The value-improvement path: Towards better representations for reinforcement learning. *CoRR*, abs/2006.02243, 2020.
- Fedus, W., Gelada, C., Bengio, Y., Bellemare, M. G., and Larochelle, H. Hyperbolic discounting and learning over multiple horizons. *CoRR*, abs/1902.06865, 2019.
- Gregor, K., Rezende, D. J., Besse, F., Wu, Y., Merzic, H., and van den Oord, A. Shaping belief states with generative environment models for RL. In Wallach, H. M., Larochelle, H., Beygelzimer, A., d’Alché-Buc, F., Fox, E. B., and Garnett, R. (eds.), *Advances in Neural Information Processing Systems 32: Annual Conference on Neural Information Processing Systems 2019, NeurIPS 2019, December 8-14, 2019, Vancouver, BC, Canada*, pp. 13475–13487, 2019.
- Guo, Z. D., Azar, M. G., Piot, B., Pires, B. A., Pohlen, T., and Munos, R. Neural predictive belief representations. *CoRR*, abs/1811.06407, 2018.
- Guo, Z. D., Pires, B. Á., Piot, B., Grill, J., Alché, F., Munos, R., and Azar, M. G. Bootstrap latent-predictive representations for multitask reinforcement learning. In *Proceedings of the 37th International Conference on Machine Learning, ICML 2020, 13-18 July 2020, Virtual Event*, volume 119 of *Proceedings of Machine Learning Research*, pp. 3875–3886. PMLR, 2020.
- Hafner, D., Lillicrap, T. P., Norouzi, M., and Ba, J. Mastering atari with discrete world models. *CoRR*, abs/2010.02193, 2020.
- Jaderberg, M., Mnih, V., Czarnecki, W. M., Schaul, T., Leibo, J. Z., Silver, D., and Kavukcuoglu, K. Reinforcement learning with unsupervised auxiliary tasks. In *5th International Conference on Learning Representations, ICLR 2017, Toulon, France, April 24-26, 2017, Conference Track Proceedings*. OpenReview.net, 2017.
- Kartal, B., Hernandez-Leal, P., and Taylor, M. E. Terminal prediction as an auxiliary task for deep reinforcement learning. In Smith, G. and Lelis, L. (eds.), *Proceedings of the Fifteenth AAAI Conference on Artificial Intelligence and Interactive Digital Entertainment, AIIDE 2019, October 8-12, 2019, Atlanta, Georgia, USA*, pp. 38–44. AAAI Press, 2019.
- Kingma, D. P. and Ba, J. Adam: A method for stochastic optimization. In Bengio, Y. and LeCun, Y. (eds.), *3rd International Conference on Learning Representations, ICLR 2015, San Diego, CA, USA, May 7-9, 2015, Conference Track Proceedings*, 2015.
- Lee, K., Fischer, I., Liu, A., Guo, Y., Lee, H., Canny, J., and Guadarrama, S. Predictive information accelerates learning in RL. In Larochelle, H., Ranzato, M., Hadsell, R., Balcan, M., and Lin, H. (eds.), *Advances in Neural Information Processing Systems 33: Annual Conference on Neural Information Processing Systems 2020, NeurIPS 2020, December 6-12, 2020, virtual*, 2020.
- Littman, M. L., Sutton, R. S., and Singh, S. Predictive representations of state. In Dietterich, T. G., Becker, S., and Ghahramani, Z. (eds.), *Advances in Neural Information Processing Systems 14 [Neural Information Processing Systems: Natural and Synthetic, NIPS 2001, December 3-8, 2001, Vancouver, British Columbia, Canada]*, pp. 1555–1561. MIT Press, 2001.

- Mazouze, B., des Combes, R. T., Doan, T., Bachman, P., and Hjelm, R. D. Deep reinforcement and infomax learning. In Larochelle, H., Ranzato, M., Hadsell, R., Balcan, M., and Lin, H. (eds.), *Advances in Neural Information Processing Systems 33: Annual Conference on Neural Information Processing Systems 2020, NeurIPS 2020, December 6-12, 2020, virtual*, 2020.
- Mnih, V., Kavukcuoglu, K., Silver, D., Rusu, A. A., Veness, J., Bellemare, M. G., Graves, A., Riedmiller, M. A., Fidjeland, A., Ostrovski, G., Petersen, S., Beattie, C., Sadik, A., Antonoglou, I., King, H., Kumaran, D., Wierstra, D., Legg, S., and Hassabis, D. Human-level control through deep reinforcement learning. *Nat.*, 518(7540):529–533, 2015. doi: 10.1038/nature14236.
- Mnih, V., Badia, A. P., Mirza, M., Graves, A., Lillicrap, T. P., Harley, T., Silver, D., and Kavukcuoglu, K. Asynchronous methods for deep reinforcement learning. In Balcan, M. and Weinberger, K. Q. (eds.), *Proceedings of the 33rd International Conference on Machine Learning, ICML 2016, New York City, NY, USA, June 19-24, 2016*, volume 48 of *JMLR Workshop and Conference Proceedings*, pp. 1928–1937. JMLR.org, 2016.
- Schwarzer, M., Anand, A., Goel, R., Hjelm, R. D., Courville, A., and Bachman, P. Data-efficient reinforcement learning with self-predictive representations. *arXiv preprint arXiv:2007.05929*, 2020.
- Singh, S., James, M. R., and Rudary, M. R. Predictive state representations: A new theory for modeling dynamical systems. In Chickering, D. M. and Halpern, J. Y. (eds.), *UAI '04, Proceedings of the 20th Conference in Uncertainty in Artificial Intelligence, Banff, Canada, July 7-11, 2004*, pp. 512–518. AUAI Press, 2004.
- Sutton, R. S. and Barto, A. G. *Reinforcement learning: An introduction*. MIT press, 2018.
- Sutton, R. S. and Tanner, B. Temporal-difference networks. In *Advances in Neural Information Processing Systems 17 [Neural Information Processing Systems, NIPS 2004, December 13-18, 2004, Vancouver, British Columbia, Canada]*, pp. 1377–1384, 2004.
- Sutton, R. S., Modayil, J., Delp, M., Degris, T., Pilarski, P. M., White, A., and Precup, D. Horde: a scalable real-time architecture for learning knowledge from unsupervised sensorimotor interaction. In Sonenberg, L., Stone, P., Tumer, K., and Yolum, P. (eds.), *10th International Conference on Autonomous Agents and Multiagent Systems (AAMAS 2011), Taipei, Taiwan, May 2-6, 2011, Volume 1-3*, pp. 761–768. IFAAMAS, 2011.
- van den Oord, A., Li, Y., and Vinyals, O. Representation learning with contrastive predictive coding. *CoRR*, abs/1807.03748, 2018.
- Veeriah, V., Hessel, M., Xu, Z., Rajendran, J., Lewis, R. L., Oh, J., van Hasselt, H., Silver, D., and Singh, S. Discovery of useful questions as auxiliary tasks. In Wallach, H. M., Larochelle, H., Beygelzimer, A., d’Alché-Buc, F., Fox, E. B., and Garnett, R. (eds.), *Advances in Neural Information Processing Systems 32: Annual Conference on Neural Information Processing Systems 2019, NeurIPS 2019, December 8-14, 2019, Vancouver, BC, Canada*, pp. 9306–9317, 2019.
- Wang, Z., Schaul, T., Hessel, M., van Hasselt, H., Lanctot, M., and de Freitas, N. Dueling network architectures for deep reinforcement learning. In Balcan, M. and Weinberger, K. Q. (eds.), *Proceedings of the 33rd International Conference on Machine Learning, ICML 2016, New York City, NY, USA, June 19-24, 2016*, volume 48 of *JMLR Workshop and Conference Proceedings*, pp. 1995–2003. JMLR.org, 2016.

A. Pseudocode for RADAR

Algorithm 1 RADAR: A Random Question Network Generator

Input: number of features n_f , discount factor γ , action set \mathcal{A} , depth D and repeat R

Output: a network G

$G \leftarrow$ an empty graph

$roots \leftarrow$ an empty set

$leaves \leftarrow$ an empty set

for $i = 1$ **to** n_f **do**

 create a new feature node f in G

$roots \leftarrow roots \cup \{f\}$

$leaves \leftarrow leaves \cup \{f\}$

 create a new prediction node v in G

$leaves \leftarrow leaves \cup \{v\}$

 add edge $\langle v, f, 1 \rangle$ to G

 add edge $\langle v, v, \gamma \rangle$ to G

end for

for $d = 1$ **to** D **do**

$expanded \leftarrow$ an empty set

for $a \in \mathcal{A}$ **do**

$parent \leftarrow$ randomly select R distinct nodes from $leaves$

for $p \in parent$ **do**

 create a new prediction node v in G

 mark v as conditioned on action a

$expanded \leftarrow expanded \cup \{v\}$

 add edge $\langle v, p, 1 \rangle$ to G

$f \leftarrow$ randomly select a node from $roots$

 add edge $\langle v, f, 1 \rangle$ to G

end for

end for

$leaves \leftarrow expanded$

end for

B. Implementation Details

B.1. Experiments on the Empty Room Environment

Neural Network Architecture. The empty room environment is fully observable and so the state representation module is a feed-forward neural network that maps the current observation O_t to a state vector S_t . It is parameterized by a 3-layer multi-layer perceptron (MLP) with 64 units in the first two layers and 32 units in the third layer. The RL module has one hidden layer with 32 units and one output head representing the state value. (There is no policy head as the policy was given). The answer network module also has one hidden layer with 32 units and one output layer. We applied a stop-gradient between the state representation module and the RL module.

Hyperparameters. Both the value function and the answer network were updated via TD. We used 8 parallel actors to generate data and updated the parameters every 8 steps. We used the Adam optimizer (Kingma & Ba, 2015) with learning rate 0.001 for all agents except the end-to-end agent which used 0.0001. The value function updates and the answer network updates used two separate optimizers with identical hyperparameters.

B.2. Atari Experiments

Neural Network Architecture. We used A2C (Mnih et al., 2016) with a standard neural network architecture for Atari (Mnih et al., 2015) as our base agent. Specifically, the state representation module consists of 3 convolutional layers. The first layer has $32 \times 8 \times 8$ convolutional kernels with a stride of 4, the second layer has $64 \times 4 \times 4$ kernels with stride 2, and the third layer has $64 \times 3 \times 3$ kernels with stride 1. The RL module has one dense layer with 512 units and two output heads for the policy and the value function respectively. The answer network has one hidden dense layer with 512 units followed by the output layer. We stopped the gradient from the RL module to the state representation module.

Hyperparameters. Following convention (Mnih et al., 2015), we used a stack of the latest 4 frames as the input to the agent, i.e., the input to the state representation module at step t is $(O_{t-3}, O_{t-2}, O_{t-1}, O_t)$. We used 16 parallel actors to generate data and updated the agent’s parameters every 20 steps. The entropy regularization was 0.01 and the discount factor for the A2C loss was 0.99. We used the RMSProp optimizer with learning rate 0.0007, decay 0.99, and $\epsilon = 0.00001$. The RL updates and the answer network updates used two separate optimizers with identical hyperparameters. The gradient from the A2C loss was clipped by global norm to 0.5. When not stopping gradient from the RL loss, we mixed the RL updates and the answer network updates by scaling the learning rate for the answer network with a coefficient c . We searched c in $\{0.1, 0.2, 0.5, 1, 2\}$ on the 6 games in the previous section. $c = 1$ worked the best for both RADAR and baseline methods.

Baseline Methods. For MHVP, we used 10 value predictions following (Fedus et al., 2019). Each prediction has a unique discount factor, chosen to be uniform in terms of their effective horizons from 1 to 100 ($\{0, 1 - \frac{1}{10}, 1 - \frac{1}{20}, \dots, 1 - \frac{1}{90}\}$). The architecture for MHVP is the same as RADAR. For PC, We followed the architecture design and hyperparameters in (Jaderberg et al., 2017). Specifically, we center-cropped the observation image to 80×80 and used 4×4 patches which resulted in 400 features. The discount factor was set to 0.9. The output of the state representation module is first mapped to a 2592-dimensional vector by a dense layer and then reshaped to a $32 \times 9 \times 9$ tensor. A deconvolutional layer then maps this 3D tensor to $|\mathcal{A}| \times 20 \times 20$ representing the action-values for each patch. We used the dueling architecture (Wang et al., 2016).

B.3. DeepMind Lab Experiments

Neural Network Architecture. For DeepMind Lab, we used the same RL module and answer network module as Atari but used a different state representation module to address the partial observability. Specifically, the convolutional layers in the state representation module were followed by a dense layer with 512 units and a GRU core (Cho et al., 2014; Chung et al., 2014) with 512 units.

Hyperparameters. We used 32 parallel actors to generate data and updated the agent’s parameters every 20 steps. The entropy regularization was 0.003 and the discount factor for the A2C loss was 0.99. We used the RMSProp optimizer with learning rate 0.0003, decay 0.99, and $\epsilon = 10^{-8}$. The RL updates and the answer network updates used two separate optimizers with identical hyperparameters. The gradient from the A2C loss was clipped by global norm to 0.5. For end-to-end (not stop-gradient) agents, we searched the mixing coefficient c in $\{0.1, 0.2, 0.5, 1, 2\}$ on *explore_goal_locations_small*, *explore_object_locations_small*, and *lasertag_three_opponents_small*. $c = 1$ worked the best for both RADAR and baseline methods.

C. Additional Empirical Results

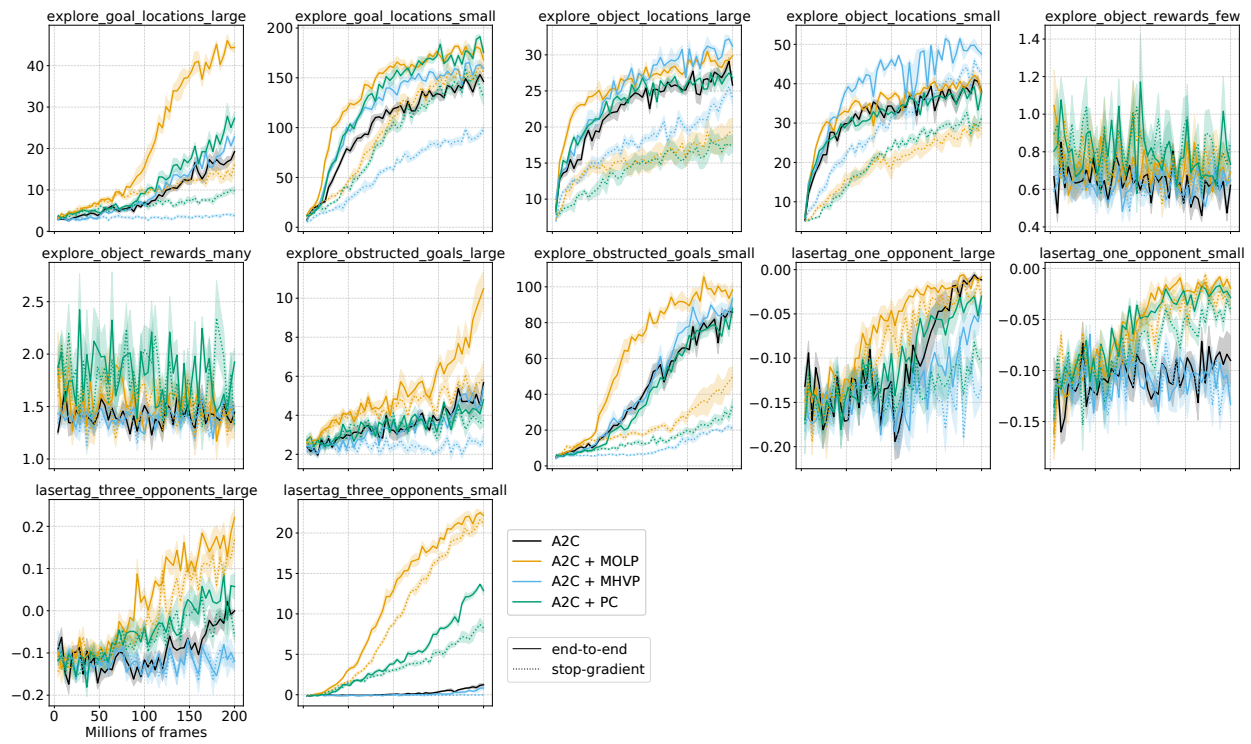


Figure 10. Learning curves in 12 DeepMind Lab environments. The x-axis denotes the number of frames. Each dark curve is averaged over 5 independent runs with different random seeds. The shaded area shows the standard error.

Learning State Representations from Random Deep Action-conditional Predictions

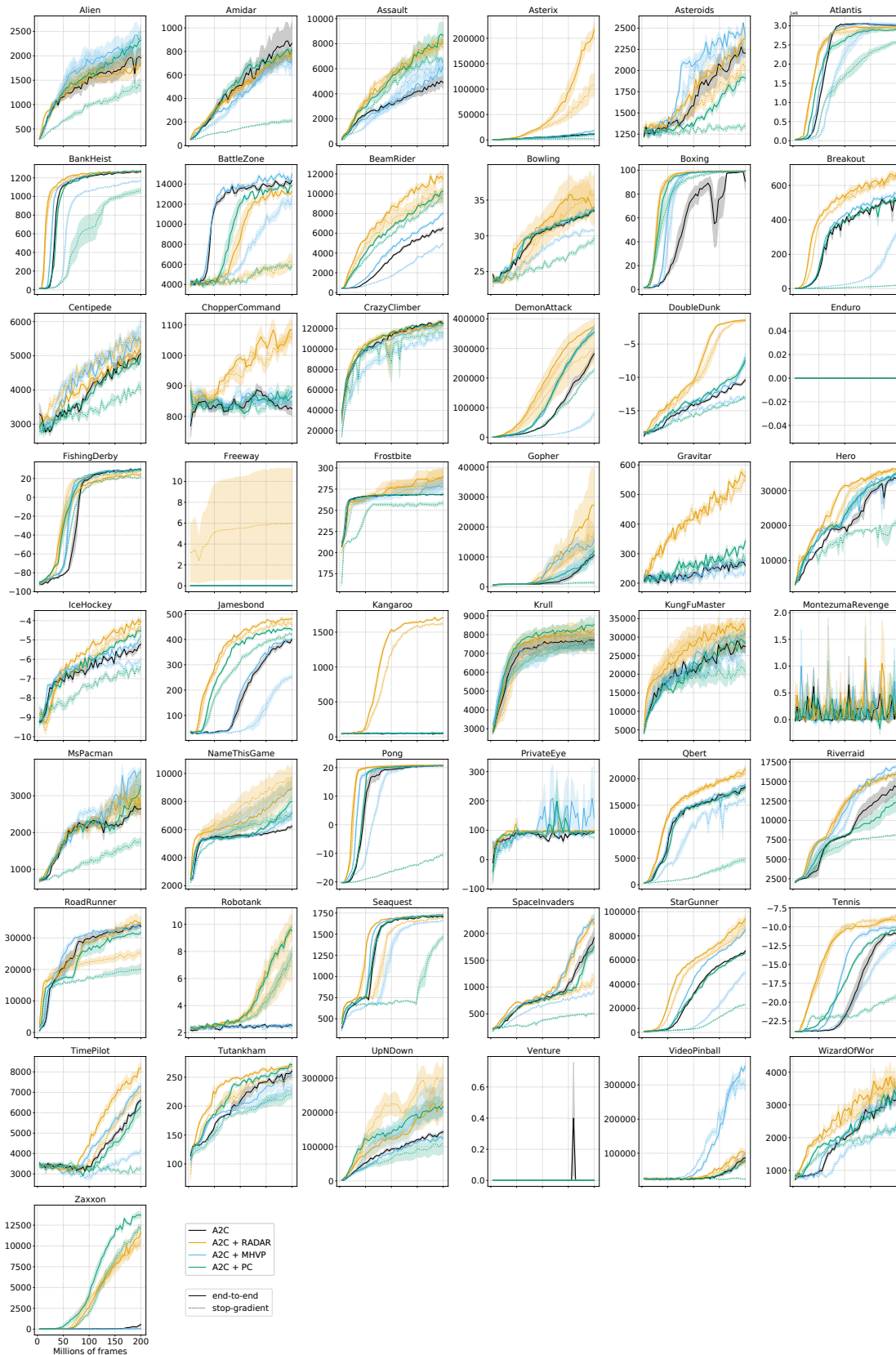


Figure 11. Learning curves in 49 Atari games. The x-axis denotes the number of frames. Each dark curve is averaged over 5 independent runs with different random seeds. The shaded area shows the standard error.